

## MODEL CALCULATION FOR THE FREQUENCY SHIFT IN CO COADSORBED WITH K ON Cu(001)

Shinichi KATSUKI, Yoshiko SAKAI

*College of General Education, Kyushu University, Fukuoka 810, Japan*

and

Eisaku MIYOSHI

*Fukuoka Dental College, Fukuoka 814, Japan*

Received 22 March 1989; accepted for publication 20 April 1989

The dramatic frequency shift recently observed for CO coadsorbed with alkali atoms on transition metals is analyzed by calculating the electronic structure of  $\text{Cu}_{12}\text{K}_2\text{CO}$  and by comparing it with that of  $\text{Cu}_{12}\text{CO}$ ,  $\text{K}_2\text{CO}$ ,  $\text{CO}^-$ , and CO at the self-consistent Hartree–Fock model-potential level. The CO vibrational frequency in the coadsorbed system is reproduced by the calculation, and the frequency shift is elucidated: it is brought about by electron redistribution which leads to reduction of the overlap population between the C and O. The electron redistribution is caused mainly by an increase of electron flow into the  $2\pi$  level due to a downward shift of this level because of direct interaction between CO and K.

### 1. Introduction

Systems in which carbon monoxide is coadsorbed with alkali atoms such as potassium have been studied extensively both theoretically and experimentally in recent years, to understand how the coadsorption of catalytic promoters affects the electronic structure of reactants [1]. Among the influences of an alkali on coadsorbed CO, the frequency shift of the C–O stretching vibrational frequency is a very dramatic one. The present work has been motivated to investigate this dramatic frequency shift which is reported to amount to more than  $500\text{ cm}^{-1}$  [1,2]. The most widely accepted model to understand the CO frequency shift on a metal surface is the Blyholder-type picture of CO bonding [3], i.e., the electron occupation of the antibonding CO  $2\pi$  level weakens the CO bond and results in a decrease in the C–O stretching frequency. This model may not be applied in the original form and a careful analysis will be needed to understand the large shifts observed upon alkali metal promotion, because the vibrational frequency of  $\text{CO}^-$ , where one extra electron occupies

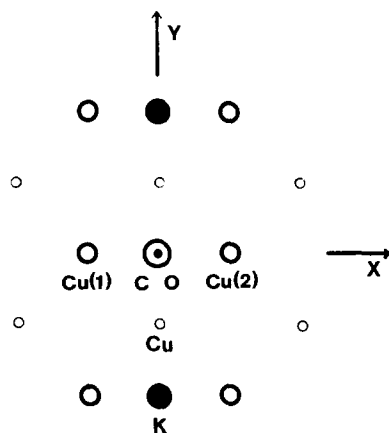


Fig. 1. The geometry of the  $\text{Cu}_{12}\text{K}_2\text{CO}$  cluster. Open circle: Cu on the first layer; small open circle: Cu on the second layer; black dot: C; large open circle: O; closed circle: K.

the  $2\pi$  orbital, has been experimentally observed to be reduced by only  $\sim 300 \text{ cm}^{-1}$  [4]. In this report we will try to elucidate how potassium atoms affect the electronic structure of CO and the CO stretching frequency shift, by calculating the electronic structure of CO coadsorbed with K on a copper surface. We adopt a cluster model, considering that the range of the alkali metal-coadsorbate interaction is primarily short range [5]. The frequency shifts will be analysed in terms of the charge density and molecular orbital contour maps and the gross and overlap population in the CO moiety by comparing them in the cases of  $\text{Cu}_{12}\text{K}_2\text{CO}$ ,  $\text{Cu}_{12}\text{CO}$ ,  $\text{K}_2\text{CO}$ ,  $\text{CO}^-$ , and CO. The  $\text{Cu}_{12}\text{K}_2\text{CO}$  cluster shown in fig. 1 is considered here as a model of the system in which CO is coadsorbed with K on Cu(001), because the most drastic frequency shift has been observed experimentally when the  $[\text{CO}]/[\text{K}]$  ratio reached 0.5 [5]. Among the CO molecular orbitals, the  $5\sigma$ ,  $1\pi$  and  $2\pi$  orbitals are the key orbitals to the CO bond change upon adsorption on a metal surface. In this geometry the  $5\sigma$  orbital belongs to the  $A_1$  irreducible representation of the  $C_{2v}$  point group, the  $1\pi_x$  and  $2\pi_x$  orbitals belong to the  $B_1$  and the  $1\pi_y$  and  $2\pi_y$  orbitals belong to the  $B_2$ . The  $1\pi_x$  and  $2\pi_x$  orbitals will be subjected to the direct influence of the copper atoms through orbital mixing between CO and  $\text{Cu}(4s)$ , since CO is adsorbed at the bridge site in this model. (A preferential filling of the bridge-bonded site by the CO adsorbate in the presence of the K has been observed experimentally [5,6].) On the other hand, the  $1\pi_y$  and  $2\pi_y$  orbitals will interact mainly with potassium orbitals. The effects caused by the copper surface and the effects caused by the potassium atoms, therefore, can be distinguished by a separate analysis of the molecular orbitals mainly composed of the CO  $\pi_x$  and  $\pi_y$  orbitals. The effect on the  $5\sigma$  is estimated by analysing the orbital belonging to the  $A_1$  irreducible representation. The

computational details for this analysis are given in section 2. Section 3 discusses the numerical results.

## 2. Computational details

We have chosen a  $\text{Cu}_{12}\text{K}_2\text{CO}$  cluster as a model to study the interaction of CO with coadsorbed K atoms and the Cu(001) surface. The cluster has  $C_{2v}$  symmetry (fig. 1). The section of bulk Cu is represented by the  $\text{Cu}_{12}$  cluster composed of two layers, each containing six atoms. The Cu–Cu nearest-neighbor distance is taken as 2.56 Å, which is the experimental value for bulk Cu [7]. The CO molecule sits at a bridge site between the central two Cu's (Cu(1) and Cu(2)); the Cu–C distance is fixed to be 2.20 Å. The two K atoms are coadsorbed at bridge sites in such a way that the K–K axis is bisected by the plane which contains Cu(1), Cu(2) and the CO molecule. The Cu–K distance is fixed to be 3.20 Å, which is the sum of the radii of single metallic bonds for the Cu and K [8].

Calculations were performed in the framework of the Hartree–Fock–Roothaan scheme by using the program package JAMOL3 [9]. In order to save computational cost, we utilized a model potential [10] for Cu and K. The model potential for Cu(1) and Cu(2) in the surface layer, to which the CO is bridge-bonded, is the sd-MP set [11]. The sd-MP set represents effects of the electrons except for the outermost 3d and 4s electrons. The model potential for the other ten Cu atoms describes the 28 “core” electrons, and only one electrons (4s) per atom is treated explicitly. We generated the model potential for K, considering 4s and 3p electrons as active electrons. The model potentials, except for the sd-MP set, are determined in the present work in a similar way as in the case of the sd-MP set. All electrons of the C and O atoms are considered as active electrons. The basis sets for C and O are taken from the work of Huzinaga et al. [12]. Basis-set contractions used in this work are as follows in the simple notation (s/p/d):

Cu(1), Cu(2): (5/1\*/41),  
 the other Cu: (5/1\*),  
 K: (41/41\*1\*),  
 C, O: (431/211),

where 1\* stands for a p-type polarization function [12].

## 3. Results and discussion

The numerical results are collected in tables 1 and 2. All orbitals and configurations of  $\text{Cu}_{12}\text{K}_2\text{CO}$ ,  $\text{Cu}_{12}\text{CO}$ ,  $\text{K}_2\text{CO}$ ,  $\text{CO}^-$ , and CO are denoted according to the irreducible representations of  $C_{2v}$  so as to make comparison

Table 1

CO stretching frequency  $\omega_e$ , bond length  $r_e$ , force constant  $\kappa$ , overlap population  $S_{CO}$  and gross population

	$\omega_e$ ( $\text{cm}^{-1}$ )	$r_e$ ( $\text{\AA}$ )	$\kappa$ ( $\times 10^6$ $\text{dyne/cm}^2$ )	$S_{CO}$	Gross population		
					C	O	Sum
CO	2339	1.13	2.21	0.99	5.73	8.27	14.00
$\text{Cu}_{12}\text{CO}$	1923	1.19	1.49	0.76	6.12	8.33	14.45
$\text{CO}^-$	1752	1.24	1.24	0.38	6.35	8.65	15.00
$\text{K}_2\text{CO}$	1673	1.24	1.13	0.24	6.11	8.69	14.80
$\text{Cu}_{12}\text{K}_2\text{CO}$	1393	1.28	0.78	0.17	6.22	8.70	14.92

easy between these five systems. In these calculations the CO stretching frequencies are obtained from potential curves calculated by moving the O atom along the C–O axis.

The C–O stretching frequency  $\omega_e$  decreases from  $2339 \text{ cm}^{-1}$  in the gas phase to  $1393 \text{ cm}^{-1}$  in the  $\text{Cu}_{12}\text{K}_2\text{CO}$  cluster, in the sequence of CO,  $\text{Cu}_{12}\text{CO}$ ,  $\text{CO}^-$ ,  $\text{K}_2\text{CO}$ , and  $\text{Cu}_{12}\text{K}_2\text{CO}$ . The CO bond distance increases from 1.13 to 1.28  $\text{\AA}$  in the same sequence. The CO frequency of  $1393 \text{ cm}^{-1}$  and the CO bond distance of 1.28  $\text{\AA}$  obtained for  $\text{Cu}_{12}\text{K}_2\text{CO}$  compare very well with the experimental values of  $1390\text{--}1420 \text{ cm}^{-1}$  (CO/K/Pt(111)) [5] and 1.27  $\text{\AA}$  (CO/Na/Pt(111)) [13]. It is worthy to remark here that the red shift in  $\text{K}_2\text{CO}$  is larger than that in  $\text{Cu}_{12}\text{CO}$  (table 1). The red shift of the CO stretching frequency and the lengthening of the CO bond are the reflection of the decrease of the C–O force constant, which is closely related to the decrease of the overlap population as seen in table 1. The red shift of the CO stretching frequency in the presence of coadsorbed K will be interpreted in terms of the decrease of the CO overlap population in the following.

The total gross population of the  $\text{CO}^-$  molecule is larger by 1.0 compared to that of the CO molecule. The extra one electron in the  $\text{CO}^-$  occupies the antibonding  $2\pi$  orbitals resulting in the decrease of the overlap population as shown in table 2. The decrease of the CO overlap population in  $\text{Cu}_{12}\text{CO}$  is due to the occupation of the CO  $2\pi_x$  orbital by the back-donated electron from the Cu surface. The back-donation arises through a lowering of the  $2\pi_x$  level

Table 2

CO overlap population

	$1\pi_x$	$1\pi_y$	$2\pi_x$	$2\pi_y$
CO	0.38	0.38	0	0
$\text{Cu}_{12}\text{CO}$	0.35	0.40	−0.39	−0.02
$\text{CO}^-$	0.34	0.34	−0.25	−0.25
$\text{K}_2\text{CO}$	0.33	0.27	0	−0.44
$\text{Cu}_{12}\text{K}_2\text{CO}$	0.31	0.28	−0.20	−0.43

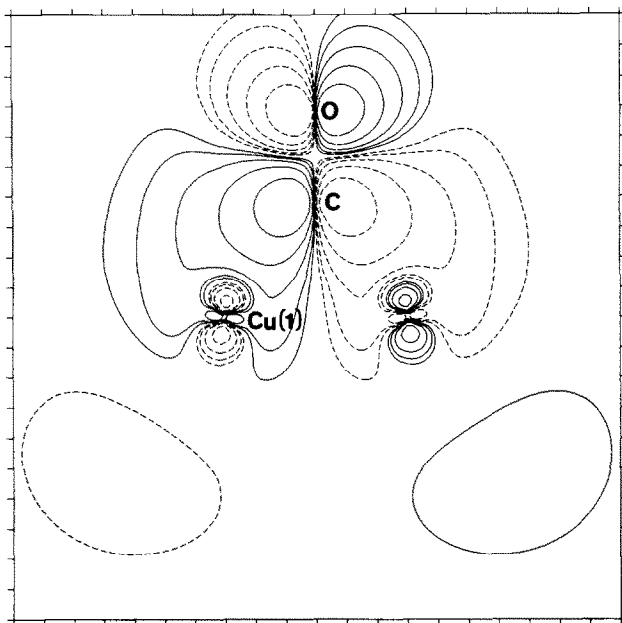


Fig. 2. The contour map of  $2\pi_x$  orbital in  $\text{Cu}_{12}\text{CO}$  in the  $x-z$  plane.

which is caused by a mixing of this orbital with the metal orbitals. As the metal orbitals participating in the mixing are those mainly composed of Cu(1) and Cu(2), the change of the overlap population occurs in the  $2\pi_x$  level (table 2). On the other hand, the decrease of the overlap population occurs in the  $2\pi_y$  level in the case of  $\text{K}_2\text{CO}$  (table 2), because the excess electron is transferred from the potassium atoms. The electron flows from K to CO through a level lowering due to mixing of the  $2\pi_y$  orbital and the potassium orbitals. Table 1 shows that the effect of K on the overlap population is larger than that of the substrate. The effect of the substrate in the case of  $\text{Cu}_{12}\text{CO}$  and the effect of the coadsorbed K in the case of  $\text{K}_2\text{CO}$  are additive in  $\text{Cu}_{12}\text{K}_2\text{CO}$  as seen in table 2 as far as the overlap population is concerned. This additive character of the effects of Cu and K is also seen by comparing the  $2\pi$  orbitals in  $\text{Cu}_{12}\text{CO}$  (fig. 2) and  $\text{K}_2\text{CO}$  (fig. 3) with those in  $\text{Cu}_{12}\text{K}_2\text{CO}$  (figs. 4 and 5). Almost the same amount of decrease of the overlap population of the  $2\pi_y$  orbitals is seen in both cases of  $\text{K}_2\text{CO}$  and  $\text{Cu}_{12}\text{K}_2\text{CO}$  (table 2). This suggests that the electron is transferred directly from K rather than through the surface, by a direct interaction between K and CO [14].

The Mulliken population analysis indicates a 1.4 electron transfer to the CO  $2\pi$  level and a backward transfer of 0.5 electrons through the  $5\sigma$  level. The  $\sigma$  and  $\pi$  electron transfer, although they are directionally opposed,

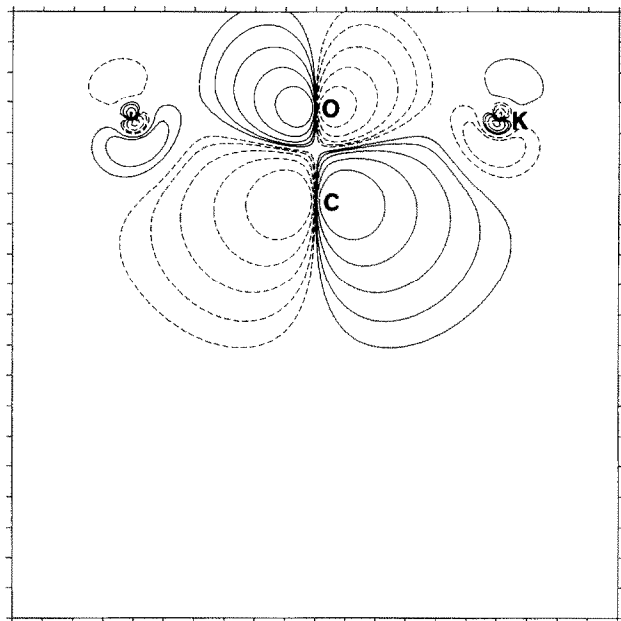


Fig. 3. The contour map of  $2\pi_y$  orbital in  $\text{K}_2\text{CO}$  in the  $y-z$  plane.

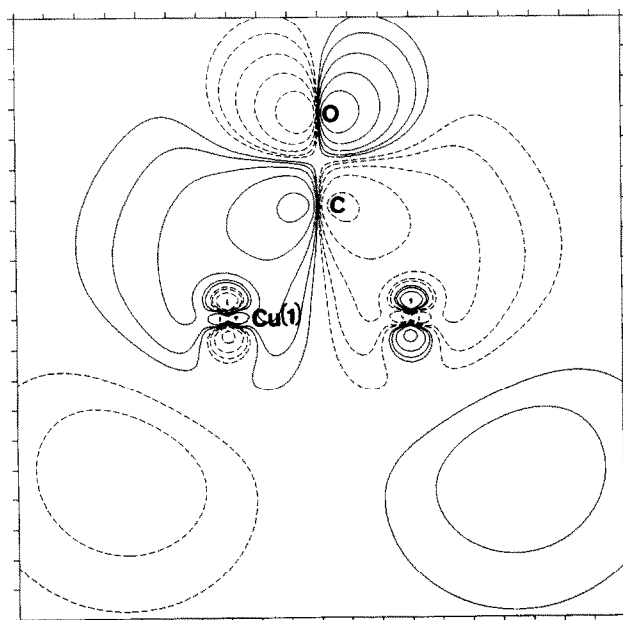


Fig. 4. The contour map of  $2\pi_x$  orbital in  $\text{Cu}_{12}\text{K}_2\text{CO}$  in the  $x-z$  plane.

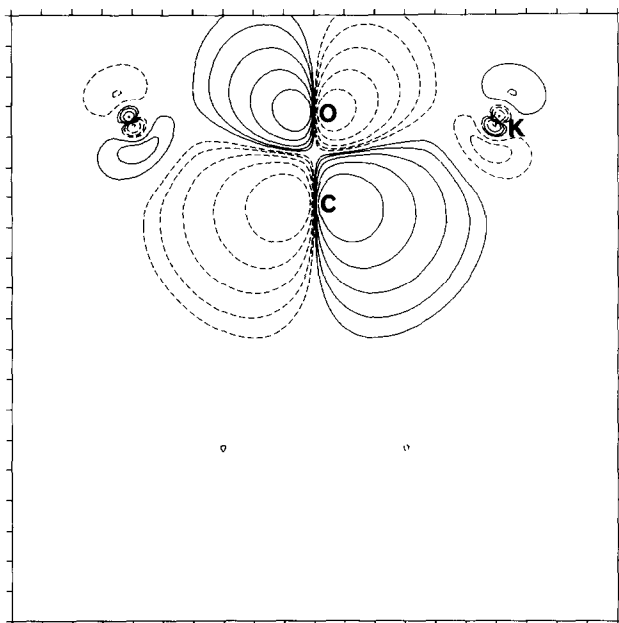


Fig. 5. The contour map of  $2\pi_y$  orbital in  $\text{Cu}_{12}\text{K}_2\text{CO}$  in the  $y-z$  plane.

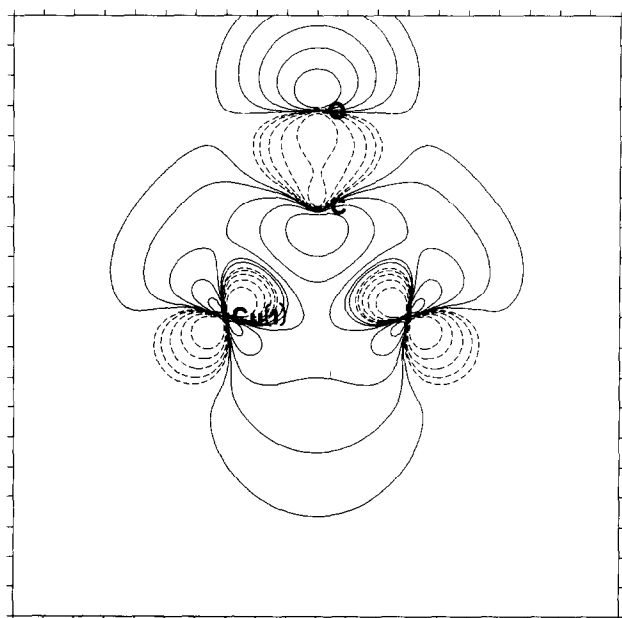


Fig. 6. The contour map of  $5\sigma$  orbital in  $\text{Cu}_{12}\text{K}_2\text{CO}$  in the  $x-z$  plane.

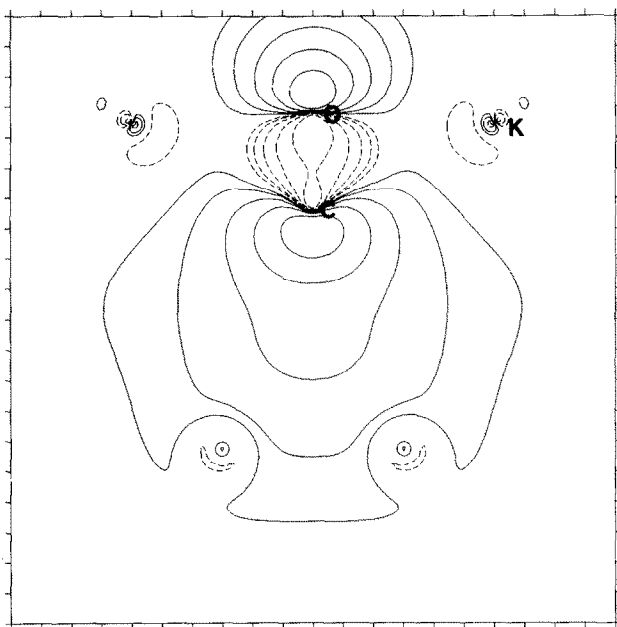


Fig. 7. The contour map of 5σ orbital in Cu<sub>12</sub>K<sub>2</sub>CO in the *y*-*z* plane.

contributes to a weakening of the CO bond [15], since the 2π orbital is of antibonding character between C and O as is already discussed and the 5σ orbital is of bonding character as shown in figs. 6 and 7. This electron flow explains why the CO overlap population in Cu<sub>12</sub>K<sub>2</sub>CO is reduced more than that in CO<sup>-</sup>, although the total gross population (14.9) in the CO moiety in Cu<sub>12</sub>K<sub>2</sub>CO is smaller than that (15.0) in CO<sup>-</sup> (table 1). The excess reduction of the CO overlap population results in a larger frequency shift in the coadsorption system than in CO<sup>-</sup>.

The change of the overlap population due to the 1π orbitals is very small compared to the drastic change due to the 2π orbital. The 1π orbital becomes polarized a little towards the O end of the CO molecule, as we can see by comparing the orbital in Cu<sub>12</sub>CO (fig. 8) with the orbitals in K<sub>2</sub>CO (fig. 9) and Cu<sub>12</sub>K<sub>2</sub>CO (figs. 10 and 11). This polarization of the 1π orbital may drive further occupation of the 2π level which weighs on the carbon end as originally suggested by Heskett et al. [16]. We cannot deny the possibility, however, that the occupation of the 2π orbital might have caused the 1π polarization.

As we have seen above, the frequency shift is brought about by electron redistribution which leads to reduction of the overlap population between C and O. The difference of the electron density between Cu<sub>12</sub>K<sub>2</sub>CO and the



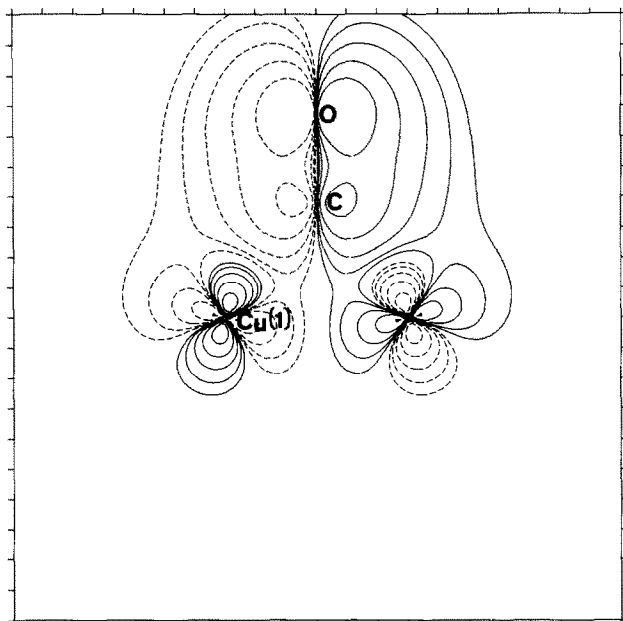


Fig. 8. The contour map of  $1\pi_x$  orbital in  $\text{Cu}_{12}\text{CO}$  in the  $x-z$  plane.

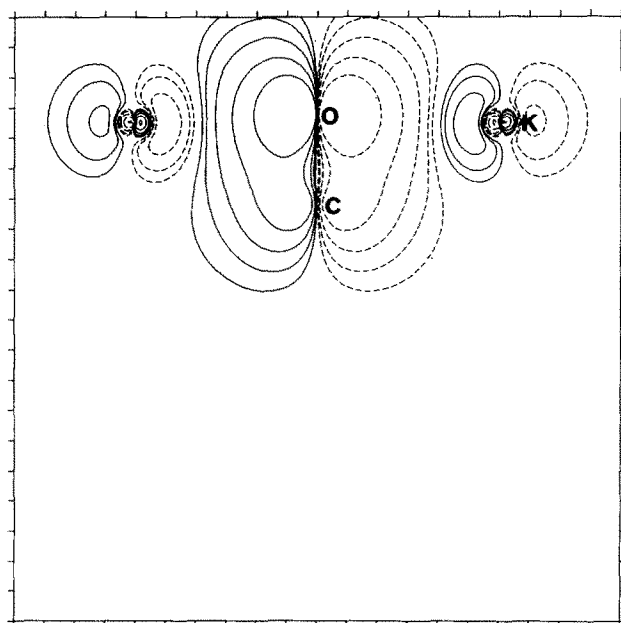


Fig. 9. The contour map of  $1\pi_y$  orbital in  $\text{K}_2\text{CO}$  in the  $y-z$  plane.

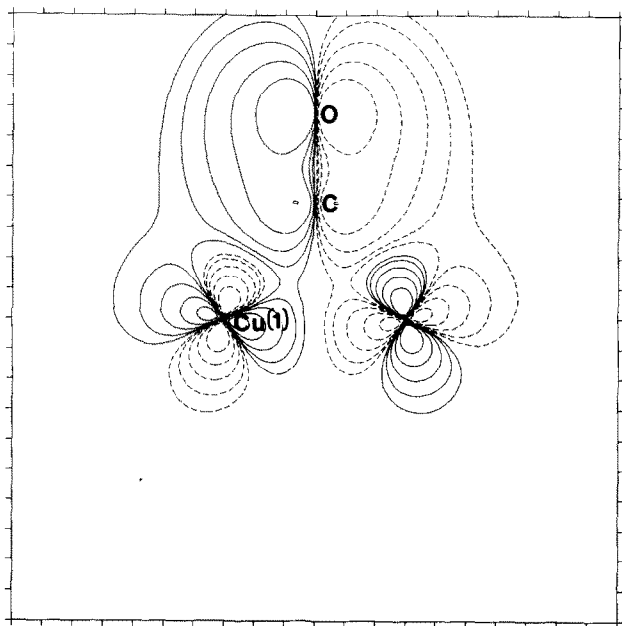


Fig. 10. The contour map of  $1\pi_x$  orbitals in  $\text{Cu}_{12}\text{K}_2\text{CO}$  in the  $x-z$  plane.

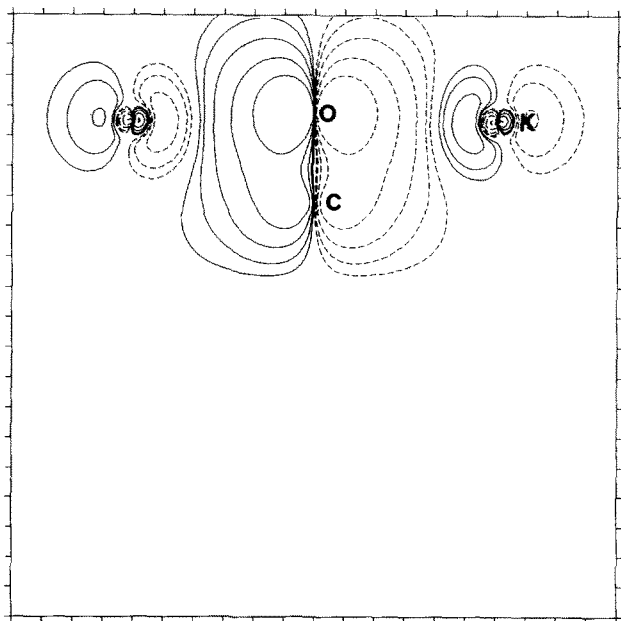


Fig. 11. The contour map of  $1\pi_y$  orbitals in  $\text{Cu}_{12}\text{K}_2\text{CO}$  in the  $y-z$  plane.

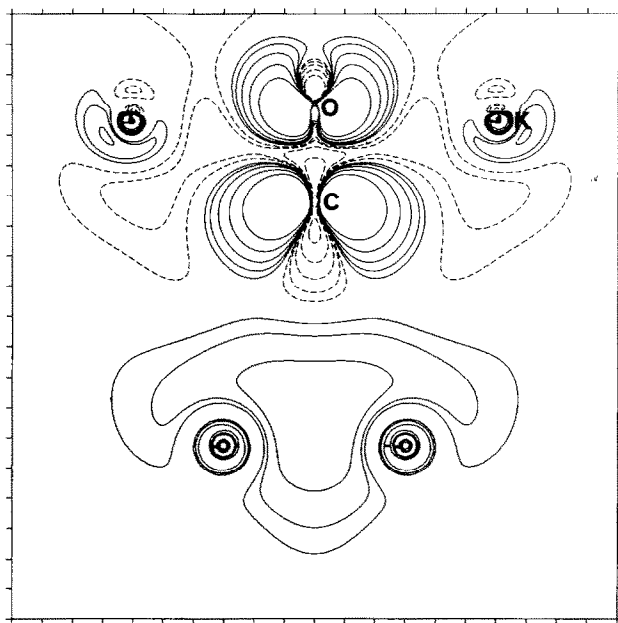


Fig. 12. The electron-density difference  $\rho(\text{Cu}_{12}\text{K}_2\text{CO}) - \rho(\text{Cu}_{12}\text{CO}) - \rho(\text{K}_2)$  in the  $y$ - $z$  plane.

system  $\text{Cu}_{12}\text{CO} + \text{K}_2$  is depicted in fig. 12. The density difference is obtained by subtracting the density in  $\text{Cu}_{12}\text{CO}$  and  $\text{K}_2$  from the density in  $\text{Cu}_{12}\text{K}_2\text{CO}$ . Fig. 12 shows how the electron density of  $\text{Cu}_{12}\text{CO}$  is rearranged under the influence of the coadsorbed potassium atoms: the electron redistribution is seen to be caused mainly by the charge density increases in the  $2\pi_y$  orbital.

In summary the drastic red shift of the CO stretching frequency has been shown to be due to the electron flow into the  $2\pi$  level (1.4 electrons) from the substrate and coadsorbed potassium atoms, and to the electron flow into the substrate (0.5 electrons) through the  $5\sigma$  level. The effect of K is larger than that of the substrate and the interaction between CO and K is direct rather than indirect through the substrate.

### Acknowledgements

The authors would like to acknowledge many valuable discussions with Drs. H. Tochihiro and H. Ueba. The numerical calculations were done at the computer centers of Kyushu University and the Institute for Molecular Science. This work was partially supported by a Grant-in-Aid for Scientific Research on Priority Areas by the Minister of Education, Science and Culture.

## References

- [1] H.P. Bonzel, Surface Sci. Rept. 8 (1987) 43.
- [2] D. Heskett, Surface Sci. 199 (1988) 67.
- [3] G. Blyholder, J. Phys. Chem. 68 (1964) 2772.
- [4] H. Ehrhardt, L. Langhans, F. Linder and H.S. Taylor, Phys. Rev. 173 (1968) 222.
- [5] G. Pirug and H.P. Bonzel, Surface Sci. 199 (1988) 371.
- [6] J.E. Crowell, E.L. Garfunkel and G.A. Somorjai, Surface Sci. 121 (1982) 303.
- [7] R.W.G. Wyckoff, Crystal Structures, 2nd ed., Vol. 1 (Wiley, New York, 1965).
- [8] L. Pauling, The Nature of the Chemical Bond (Cornell Univ. Press, New York, 1960).
- [9] H. Kashiwagi, T. Takada, E. Miyoshi, S. Obara and F. Sasaki, A program package JAMOL3 for SCF-MO calculations.
- [10] Y. Sakai, J. Chem. Phys. 75 (1981) 1303;  
Y. Sakai and S. Huzinaga, J. Chem. Phys. 76 (1982) 2537, 2552.
- [11] Y. Sakai, E. Miyoshi, M. Klobukowski and S. Huzinaga, J. Comput. Chem. 8 (1987) 226.
- [12] S. Huzinaga, J. Andzelm, M. Klobukowski, E. Radzio-Andzelm, Y. Sakai and H. Tatewaki, Gaussian Basis Sets for Molecular Calculations (Elsevier, Amsterdam, 1984).
- [13] F. Sette, J. Stohr, E.B. Kollin, D.J. Dwyer, J.L. Gland, J.L. Robbins and A.L. Johnson, Phys. Rev. Letters 54 (1985) 935.
- [14] P.A. Schulz, C.H. Patterson and R.P. Messmer, J. Vacuum Sci. Technol. A 5 (1987) 1061.
- [15] B. Silvi, O. Ayed and W.B. Person, J. Am. Chem. Soc. 108 (1986) 8148.
- [16] D. Heskett, I. Strathy, E.W. Plummer and R.A. de Paola, Phys. Rev. B 32 (1985) 6222.